

1 **Quantitative analysis of SARS-CoV-2 RNA from wastewater solids in communities**
2 **with low COVID-19 incidence and prevalence**

3 Patrick M. D'Aoust¹, Élisabeth Mercier³, Danika Montpetit³, Jian-Jun Jia¹, Ilya Alexandrov⁴, Nafisa
4 Neault², Aiman Tariq Baig², Janice Mayne⁵, Xu Zhang⁵, Tommy Alain^{2,5}, Mark R. Servos⁸, Malcolm
5 MacKenzie⁴, Daniel Figeys⁵⁻⁷, Alex E. MacKenzie², Tyson E. Graber², Robert Delatolla^{1*}

6 1: Department of Civil Engineering, University of Ottawa, Ottawa, Canada, K1N 6N5
7 2: Children's Hospital of Eastern Ontario Research Institute, Ottawa, Canada, K1H 8L1
8 3: Department of Chemical Engineering, University of Ottawa, Canada, K1N 6N5
9 4: ActivSignal LLC., 27 Strathmore Rd Natick, MA, United States, 01760
10 5: Department of Biochemistry, Microbiology and Immunology, University of Ottawa, Ottawa, Canada,
11 K1H 8M5
12 6: Department of Chemistry and Biomolecular Sciences, University of Ottawa, Ottawa, Canada, K1N 6N5
13 7: Canadian Institute for Advanced Research, Toronto, ON, M5G 1M1
14 8: Department of Biology, University of Waterloo, Waterloo, Canada, N2L 3G1
15

16 Corresponding author:

17 **Dr. Robert Delatolla**

18 Associate Professor

19 Work E-mail: robert.delatolla@uOttawa.ca

20 Abstract

21 In the absence of an effective vaccine to prevent COVID-19 it is important to be able to track
22 community infections to inform public health interventions aimed at reducing the spread and therefore
23 reduce pressures on health-care units, improve health outcomes and reduce economic uncertainty.
24 Wastewater surveillance has rapidly emerged as a potential tool to effectively monitor community
25 infections for severe acute respiratory syndrome coronavirus 2 (SARS-CoV-2), through measuring trends
26 of viral RNA signal in wastewater systems. In this study SARS-CoV-2 viral RNA N1 and N2 genes are
27 quantified in solids collected from influent post grit solids (PGS) and primary clarified sludge (PCS) in two
28 water resource recovery facilities (WRRF) serving Canada's national capital region, i.e., the City of
29 Ottawa , ON (pop. \approx 1.1M) and the City of Gatineau, QC (pop. \approx 280K). PCS samples show signal
30 inhibition using RT-ddPCR compared to RT-qPCR, with PGS samples showing similar quantifiable
31 concentrations of RNA using both assays. RT-qPCR shows higher frequency of detection of N1 and N2
32 genes in PCS (92.7, 90.6%) as compared to PGS samples (79.2, 82.3%). Sampling of PCS may
33 therefore be an effective approach for SARS-CoV-2 viral quantification, especially during periods of
34 declining and low COVID-19 incidence in the community. The pepper mild mottle virus (PMMV) is
35 determined to have a less variable RNA signal in PCS over a three month period for two WRRFs,
36 regardless of environmental conditions, compared to *Bacteroides* 16S rRNA or human eukaryotic 18S
37 rRNA, making PMMV a potentially useful biomarker for normalization of SARS-CoV-2 signal. PMMV-
38 normalized PCS RNA signal from WRRFs of two cities correlated with the regional public health
39 epidemiological metrics, identifying PCS normalized to a fecal indicator (PMMV) as a potentially effective
40 tool for monitoring trends during decreasing and low-incidence of infection of SARS-Cov-2 in
41 communities.

42 **Keywords:** COVID-19; SARS-CoV-2; wastewater; primary clarified sludge; solids; water resource
43 recovery facility

44 **1. Introduction**

45 Since the onset of the novel coronavirus disease in 2019 (COVID-19), the rapid transmission and
46 global spread of the disease has placed significant strain on public health agencies around the world.
47 Detection of SARS-CoV-2 RNA in nasopharyngeal (NP) swab specimens by reverse transcription
48 quantitative polymerase chain reaction (RT-qPCR) is the standard diagnostic test to confirm COVID-19.
49 Accurately measuring the prevalence of COVID-19 in many countries has been complicated by limited
50 and/or biased NP testing (targeting symptomatic groups) and an asymptomatic, or mildly symptomatic
51 infectious period in a significant proportion of cases (Long et al., 2020; Pan et al., 2020). Additional
52 detection tools are thus desirable to mitigate these challenges and provide public health agencies and
53 governments new metrics to help guide their implementation of societal restrictions (Daughton, 2009; Hill
54 et al., 2020; Thompson et al., 2020).

55 Recent systematic reviews and meta-analyses of the current peer-reviewed and preprint literature
56 confirm fecal SARS-CoV-2 viral RNA detection in roughly half of COVID-19 patients (Gupta et al., 2020;
57 Parasa et al., 2020). Moreover, a systematic review and meta-analysis of SARS-CoV-2 viral RNA
58 detection profiles in several different types of COVID-19 patient specimens found that positive detection
59 rates were higher in rectal and sputum swabs than in the commonly used NP swab (Bwire et al., 2020).
60 These data provide a clear rationale to probe wastewater for SARS-CoV-2 RNA.

61 Medema et al. (2020) first reported the detection of SARS-CoV-2 viral RNA in wastewater from
62 WRRFs located in seven different cities in the Netherlands. SARS-CoV-2 viral RNA has subsequently
63 been identified and is being monitored at numerous WRRFs around the world (Ahmed et al., 2020a;
64 Alpaslan-Kocamemi et al., 2020; Bar Or et al., 2020; Haramoto et al., 2020; La Rosa et al., 2020;
65 Medema et al., 2020; Nemudryi et al., 2020; Peccia et al., 2020a; Randazzo et al., 2020; Rimoldi et al.,
66 2020; Wu et al., 2020; Wurtzer et al., 2020; Zhang et al., 2020) The successful monitoring of the viral
67 signal has led the Netherlands (National Institute for Public Health and the Environment, 2020), Australia
68 (Dalzell, 2020), Germany (Pleitgen, 2020) and Finland (Yle, 2020) to plan and implement national
69 wastewater surveillance programs for SARS-CoV-2 as a viral tracking tool to complement existing public

70 health metrics. There are also early and promising indications from several research groups that
71 wastewater surveillance of SARS-CoV-2 might be predictive, providing earlier warning of community
72 outbreak than current NP-based PCR diagnostics.

73 Although studies reported some success in the detection and even quantitation of SARS-CoV-2
74 RNA by RT-qPCR in wastewaters over the course of community COVID-19 outbreaks, poor assay
75 sensitivity and systematic variation represent significant challenges, particularly in regions with low
76 COVID-19 prevalence (Bar-On et al., 2020; Michael-Kordatou et al., 2020; Orive et al., 2020; Randazzo
77 et al., 2020). Specifically, monitoring in communities with low incidence has demonstrated high PCR Ct
78 values and hence variable or unquantifiable data being collected due to very low concentrations of the
79 viral fragments in wastewaters. In this regard, at least two groups have identified improved sensitivity in
80 solids-rich wastewater samples collected from WRRFs in communities with low incidence and prevalence
81 (<25 active cases/100,000 population) (Balboa et al., 2020; Peccia et al., 2020b, 2020a). However, it has
82 been observed that due to variations both in case numbers and influent wastewater sample data
83 (Medema et al., 2020; Wu et al., 2020), studies have so far reported high day to day variance and noise
84 (Balboa et al., 2020; Peccia et al., 2020a); which is a key challenge in establishing trends and extracting
85 meaningful information from SARS-CoV-2 wastewater sentinel surveillance programs to date.

86 This study investigates and optimizes the detection of SARS-CoV-2 RNA in wastewater influent
87 solids (post-grit solids; PGS) and primary clarified sludge (PCS) in two municipal WRRFs serving Ottawa
88 and Gatineau beginning after the height of the epidemic with a period (April to May 2020) characterized
89 by decreasing COVID-19 incidence and a subsequent period (May to June 2020) of low COVID-19
90 prevalence. Using both RT-qPCR and RT-droplet digital (dd) PCR, rigorous quality control metrics are
91 applied to compare the detection sensitivity of viral N1 and N2 RNA in PGS compared to PCS using two
92 different established primer/probe sets. Furthermore, the study tests the human microbiome-specific
93 HF183 *Bacteroides* 16S ribosomal RNA (rRNA) the eukaryotic 18S rRNA and pepper mild mottle virus
94 (PMMV) RNA as reliable and robust nucleic acid normalization biomarkers that can be used to control
95 systematic noise associated with variances in WRRF daily operations, sampling, storage, processing and
96 analysis of the samples. Finally, the study compares and correlates biomarker normalized longitudinal

97 data sets of the two municipalities with epidemiological metrics to evaluate the usefulness of SARS-CoV-
98 2 viral measurements in wastewater as a complimentary tool to clinical testing in a community during
99 decreasing and low COVID-19 incidence.

100 2. Materials and methods

101 2.1. Characteristics of the City of Ottawa and Gatineau WRRFs

102 Post-grit chamber influent solids and primary clarified sludge samples were collected from the
103 City of Ottawa's Robert O. Pickard Environmental Centre, Ontario and the City of Gatineau, Quebec
104 water resource recovery facilities (WRRFs). The two facilities are located across the Ottawa River from
105 each other in the national capital region of Canada (Figure 1). The two WRRFs service over 1.3 million
106 people, or approximately 3.7% of Canada's total population. The sewershed of the City of Ottawa WRRF
107 services approximately 1.1M people and the sewershed of the city of Gatineau WRRF services

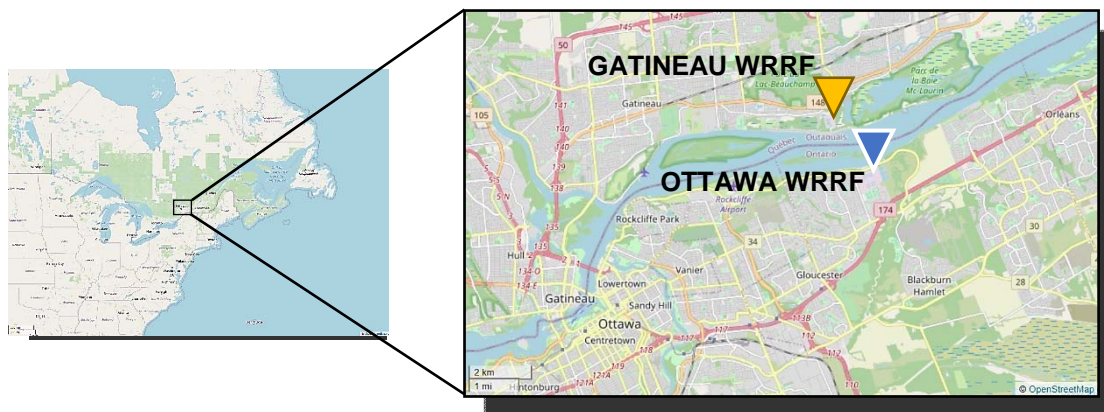


Figure 1. Location of the city of Ottawa and Gatineau WRRFs.

108 approximately 280K people.

109 Ottawa and Gatineau WRRFs are designed and operated as conventional activated sludge
110 treatment systems (Table 1). The grit chambers of both facilities, where a portion of the samples are
111 collected in this study, are located toward the front of both WRRF treatment trains and are fed by coarse
112 and fine screened wastewaters. The grit chambers of both facilities subsequently feed the primary

113 clarifiers, where remaining portion of the samples are collected in this study. The hydraulic residence time
114 of the Ottawa sewershed ranges from 2 hours to 35 hours, with an average residence time of
115 approximately 12 hours. In comparison, the hydraulic residence time of Gatineau's sewershed ranges
116 from 2 hours to 7 hours, with an average of approximately 4 hours.

117 Table 1: Characteristics of surveyed WRRFs

Facility Parameter	Ottawa WRRF (ROPEC)	Gatineau WRRF
Average daily flow (m ³ /day)	435,000	148,890
Treatment level	Secondary	Secondary
Preliminary treatment	Coarse screens, fine screens, grit chamber	Coarse screens, fine screens, grit chamber
Primary treatment	Covered rectangular primary clarifiers	Open-air circular primary clarifiers
Secondary treatment	Conventional activated sludge	Conventional activated sludge
Disinfection prior to discharge	Chlorination	UV
Notes	BOD removal without nitrification	BOD removal, nitrification during warmer months

118

119 2.2. Wastewater sampling and analysis

120 2.2.1. PGS samples

121 Fourteen and nine 24-hour composite PGS samples were analyzed from the Ottawa and
122 Gatineau WRRFs, respectively. Clean 250 mL HDPE sampling bottles were sanitized with a 10% bleach
123 solution and then washed with RNase AWAY™ (ThermoFisher, Ottawa, Canada), rinsed with deionized
124 water, and sealed. The PGS samples in this study are collected in the stream exiting the grit chambers.
125 These samples have large debris removed via screens as was the dense grit via the grit chamber. A bio-
126 banked wastewater influent sample from a nearby WRRF collected in August 2019 was utilized as a
127 SARS-COV-2 negative control (Supplemental Figure S1).

128 250 mL hourly composite samples were collected over a 24-hour period (for a total of 6 L) using
129 an ISCO autosampler (Hoskin Scientific, Burlington, Canada) that collects directly from the exit stream of
130 the grit chamber units at both facilities. The samples in the ISCO autosamplers were maintained at
131 approximately 4°C during sampling with the frequent addition of ice (with a maximum recorded
132 temperature of 7°C across the study). Starting in June, the ISCO autosamplers were linked to

133 refrigerators, allowing the samples to be kept at temperatures of approximately 2°C immediately upon
134 collection. The harvested samples were transported from the WRRFs to the laboratory in coolers packed
135 on ice and were immediately refrigerated at 4°C for a maximum of 24 hours prior to analysis.

136 **2.2.2. PCS samples**

137 For the first 55 days of the study, grab samples of PCS were collected every second week at the
138 Ottawa and Gatineau WRRFs. These sludge samples were harvested from the primary sludge streams in
139 the two facilities at the manifold where the primary clarified sludge that exits all primary clarifiers was
140 mixed into a single stream. From day 56 onward, with the stronger RNA signal detected in PCS samples
141 as compared to PGS samples, 24-hour composite PCS samples were collected by plant process
142 technicians every other day at the Ottawa facility. The 24-hour composite samples collected at the Ottawa
143 WRRF were comprised of four grab samples collected every 6 hours. Upon collection, samples were
144 stored on-site at the Ottawa facility at 4°C in a refrigerator until mixed to form daily 24-hour composite
145 samples and transported on ice to the laboratory the subsequent day. All samples were stored at 4°C at
146 the laboratory and processed within 6 hours of arrival. Samples which could not immediately be analyzed
147 were stored at 4°C for a maximum of 24 hours prior to analysis in the laboratory. Meanwhile, in Gatineau,
148 an ISCO autosampler was linked to a refrigerator and was connected to a PCS sampling port. The
149 autosampler collected hourly grab samples of 250 mL, which were subsequently mixed to form a 24-hour
150 composite sample. Due to the size differences of the two facilities in this study and the available
151 resources at the two facilities during the COVID-19 pandemic in Canada, the Gatineau facility sampling
152 frequency was limited to a maximum of once a week as opposed to every second day as was performed
153 at the larger Ottawa facility. The 24-hour composite samples were collected and transported on ice to the
154 laboratory as outlined for the Ottawa samples.

155 2.2.3. Wastewater quality characterization of samples

156 The following PGS and PCS sample wastewater quality constituents were analyzed upon
157 collection: biological oxygen demand (BOD) (5210 B) (APHA, WEF, 2012), chemical oxygen demand
158 (COD) (SM 5220 D) (APHA, WEF, 2012), total suspended solids, volatile suspended solids, total solids
159 and total volatile solids (TSS, VSS, TS & VS) (SM 2540 D, E & B) (APHA, WEF, 2012), total ammonia
160 nitrogen (TAN) (SM 4500-C) (APHA, 1989). Dissolved oxygen (DO) and pH values were measured on-
161 site during collection of samples with a YSI ProODO (Yellow Springs, FL) and HACH PHC201/HACH
162 HQ40d probe/meter combo (Loveland, CO).

163 2.3. SARS-CoV-2 concentration

164 A preliminary study was first performed on partitioned 24-hour composite PGS samples to identify
165 fractions with SARS-CoV-2 RNA positivity (Figure 2). The 6 L, 24-hour composite PGS samples were first
166 settled at 4°C for an hour. The supernatant was subsequently decanted and serially filtered through a 1.5
167 µm glass fiber filter (GFF) followed by a 0.45 µm GF6 mixed cellulose ester (MCE) filter (filtrate fraction).
168 An eluate fraction was then collected by passing 32 mL of elution buffer (0.05 M KH₂PO₄, 1.0 M NaCl, 0.1
169 % (v/v) Triton X-100, pH 9.2) through the spent filters. Each of the three fractions were subsequently

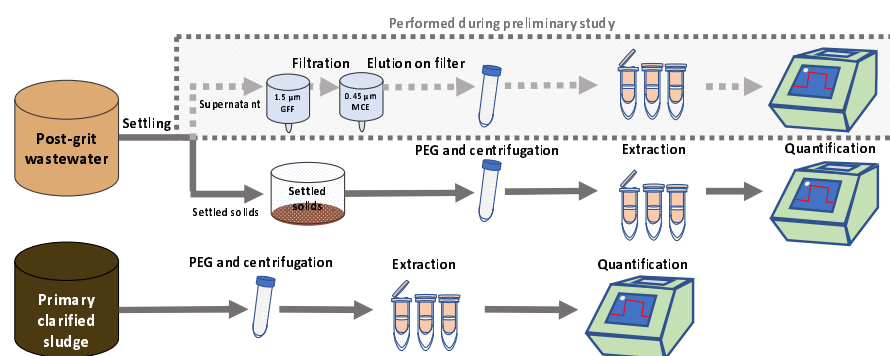


Figure 2: Flowchart showing sample work-up and processing for PGS and PCS, including RNA concentration, extraction and quantification.

170 PEG-concentrated and extracted and analyzed for SARS-CoV-2 RNA.

171 To concentrate viral particles, nucleic acids, and proteins, 32 mL of PGS or PCS was precipitated
172 with polyethylene glycol (PEG) 8000 at a final concentration of 80 g/L and 0.3M g/L NaCl, pH 7.3 and in a
173 final volume of 40 mL (Comelli et al., 2008; Petterson et al., 2015). Samples were then agitated at 4°C on
174 an orbital shaker set at 160 RPM for a period of 12 to 17 hours, then centrifuged at 10,000 x g for 45
175 minutes at 4°C. The supernatant was decanted, being careful to preserve any pellet. Samples were then
176 centrifuged a second time at 10,000 x g for another 10 minutes and the remaining supernatant decanted.
177 The resulting PCS and PGS pellets were transferred to a new RNase-free centrifuge tube and frozen at -
178 80°C until RNA extraction.

179 **2.4. RNA extraction**

180 Viral RNA was extracted from PGS and PCS samples using the RNeasy PowerMicrobiome Kit
181 (Qiagen, Germantown, MD), with the following deviations from the manufacturer's recommended
182 protocol: i) 200 mg of sample pellet was added to the initial extraction step in place of 200 µL of liquid
183 sample, and ii) the optional phenol-chloroform mixture addition to the lysis buffer was substituted with
184 Trizol LS reagent (ThermoFisher, Ottawa, Canada) to maximize lysis of cells/virion encapsulated
185 fragments and protect RNA prior to vortexing and centrifugation. The resulting aqueous phase of the lysis
186 procedure was then retained and processed as per the recommended protocol including the on-column
187 enzymatic DNA removal step. RNA was eluted in 100 µl of RNase-free water.

188 **2.5. Viral recovery efficiency**

189 An important metric in the quantification of viral signal in wastewater is the process recovery
190 efficiency for targets of interest, as it facilitates a comparison of results from study to study, even if
191 different sample processing or extraction methodologies/techniques are used. In this study, the efficiency
192 of virus recovery following the fractionation, PEG concentration and RNA extraction process was
193 determined by spiking vesicular stomatitis virus (VSV) and quantifying the recovered quantities of virus
194 after sample processing. Spiking samples with a human coronavirus with low pathogenicity such as
195 HCoV-229E as a recovery control (Gundy et al., 2009) was desirable but not practical due to the relative

196 difficulty of its procurement in Canada at the time of this study and the difficulty of propagating
197 coronaviruses in vitro. VSV is an enveloped, single stranded negative-sense RNA virus belonging to the
198 *Rhabdoviridae* family, genus *Vesiculovirus* (Letchworth et al., 1999). The RNA genomes of both VSV and
199 SARS-CoV-2 are encapsulated by a lipid envelope, and their particle sizes are similar; with VSV ranging
200 from 70-200 nm (Cureton et al., 2010) and SARS-CoV-2 being approximately 100 nm (Supplemental
201 Figure S2) (Bar-On et al., 2020). It was reasoned that these similar biophysical characteristics (lipid
202 envelope and particle size) would lead both viruses to associate with wastewater matrices and to be
203 precipitated with PEG with similar efficiencies. To maximize safety of the method, VSV was heat
204 inactivated at 55°C for five minutes prior to use (Supplemental Figure S3).

205 Recovery efficiency was quantified twice during this study, following procedures similar to those
206 outlined in Annex G of ISO 15216-1:2017 (ISO, 2017; Lowther et al., 2019; Randazzo et al., 2020). VSV
207 was quantified via RT-ddPCR for both PGS and PCS from triplicate, serial dilutions of 5.5×10^4 , 5.5×10^5 ,
208 5.5×10^6 and 5.5×10^7 copies VSV/ μ L of inactivated stock VSV culture spiked into the collected PGS
209 samples and the PCS samples. Throughout the study, quantified quantities were not corrected for
210 process extraction efficiency or for PCR inhibition. Three PCS and PGS samples were each spiked with
211 10 μ L aliquots of 5.5×10^4 , 5.5×10^5 , 5.5×10^6 and 5.5×10^7 copies/ μ L. These samples were directly
212 concentrated, extracted and quantified using RT-qPCR. The probes and primers used are listed in
213 Supplemental Table S3. The VSV recovery efficiency (mean and standard deviation) was calculated
214 based on the number of copies quantified using RT-qPCR. The equation for the calculations is as follows:

215 Eq. 1:
$$\text{Viral recovery efficiency (\%)} = \frac{\text{Total VSV gene copies recovered}}{\text{Total VSV gene copies spiked in grit/sludge}} * 100\%$$

216 2.6. Variance of biomarkers for normalization

217 Analysis of variance was used to identify biomarkers with low variability and higher temporal
218 consistency. The analysis of variance was conducted on 30 PGS and PCS samples over a period of 55
219 days (between April 8th 2020 and June 2nd 2020). The samples were analyzed for the following three
220 internal normalization biomarkers: i) human microbiome-specific HF183 *Bacteroides* 16S ribosomal rRNA,
221 ii) eukaryotic 18S rRNA and iii) PMMV.

222 **2.7. RT-qPCR**

223 Preliminary testing of samples with the CDC N1, N2 and N3 primer-probe sets and the Sarbeco
224 E-gene primer-probe set (Supplemental Table S3) demonstrated best detection and least variance in
225 technical replicates with the CDC N1 and N2 primer-probe sets. Singleplex, probe-based, one-step RT-
226 qPCR (Reliance One-Step Multiplex RT-qPCR Supermix (Bio-Rad, Hercules, CA) was performed in this
227 study using the 2019-nCoV Assay-RUO probe/primers mixes for CDC N1 and N2 gene regions (IDT,
228 Kanata, Canada). All utilized primer/probe sets, their sequences and their sources (including PMMV and
229 VSV) are described below in Supplemental Table 3. Reactions were comprised of 1.5 µl of RNA template
230 input, 500 nM each of forward and reverse primers along with 125 nM of the probes in a final reaction
231 volume of 10 µl. Samples were run in triplicate. Using a CFX Connect qPCR thermocycler (Bio-Rad,
232 Hercules, CA), RT was performed at 50°C, 10 minutes, followed by polymerase activation at 95°C for 10
233 minutes, and 45 cycles of denaturation, annealing/extension at 95°C/10 s, then 60°C/30 s, respectively.
234 Serial dilutions of the viral RNA standard were run on every 96-well PCR plate to produce standard
235 curves used to quantify the copies of SARS-CoV-2 genes. In addition, RT-ddPCR-quantified pooled
236 samples of RNA template were serial diluted and utilized to construct standard curves for PMMV
237 normalization biomarker when RNA signal was normalized by the concentration of PMMV. Additionally,
238 RT-qPCR runs were validated with the use of non-template-controls (NTCs), positive controls, negative
239 controls of pre-COVID 19 pandemic wastewater samples and dilutions.

240 The limit of detection of the RT-qPCR assay was determined for N1 and N2 gene regions, by
241 determining the number of copies per reaction which corresponds to a detection rate of $\geq 95\%$ (<5% false
242 negatives), as recommended by the MIQE guidelines (Bustin et al., 2009). Furthermore, samples were
243 discarded if they did not meet the following conditions: i) standard curves with $R^2 \geq 0.95$, ii)
244 copies/reaction are in linear dynamic range of the curve and iii) primer efficiency between 90%-130%.
245 Furthermore, sample replicates with values greater than 2 standard deviations from the mean of the
246 triplicates were also identified as possible anomalies in this study and discarded.

247 **2.8. RT-ddPCR**

248 Singleplex, probe-based, one-step RT-ddPCR (1-Step RT-ddPCR Advanced Kit for Probes, Bio-
249 Rad, Hercules, CA) was used for absolute quantification of SARS-CoV-2 N RNA in wastewaters using the
250 CDC N1, N2 or N3 primer-probe sets, or E RNA expression, using the Sarbeco E-gene primer-probe set
251 (Supplemental Table S3). Primers and probes used in this study were obtained from Integrated DNA
252 Technologies, Inc (IDT, Kanata, Canada) and ThermoFisher. 5 μ l of RNA template, 900 nM each of
253 forward and reverse primers and 250 nM of the probe together with the supermix were assembled in a
254 final reaction volume of 20 μ l. Samples were prepared and run in triplicate. Droplet generation was
255 performed using a QX200 droplet generator (Bio-Rad, Hercules, CA). Droplets were transferred to a new
256 microplate, and PCR was completed in a C1000 (Bio-Rad, Hercules, CA) thermocycler as follows:
257 reverse transcriptase (RT) was performed at 50°C, 60 minutes, followed by polymerase activation at 95°C
258 for 10 minutes, and 40 cycles of denaturation, annealing/extension at 94°C/30 s, then 55°C/60 s,
259 respectively. The polymerase was deactivated at 98°C for 10 minutes and droplets stabilized at 4°C for 30
260 minutes. Droplets were then read using a QX200 droplet reader (Bio-Rad, Hercules, CA). Positive
261 droplets were called manually, and absolute quantification was performed using Quantasoft Analysis Pro
262 v.1.0 (Bio-Rad, Hercules, CA). The limit of detection of the RT-ddPCR assay was determined for N1 and
263 N2 gene regions by determining the number of copies per reaction which corresponds to a detection rate
264 of $\geq 95\%$ (<5% false negatives), as recommended by the MIQE guidelines (Bustin et al., 2009).

265 **2.9. Statistical analysis**

266 In order to test for significant differences between data sets comparing the detection of SARS-
267 CoV-2 in PGS and PCS samples, chi-square and Fisher's exact test statistical analyses were conducted
268 using GraphPad's Prism 8.3 software (La Jolla, CA). A student's t-test was used to test for statistical
269 differences between detection of RNA in RT-qPCR and RT-ddPCR assays for PGS and PCS. A student's
270 t-test and Pearson's correlation analyses were performed to test for significance and the strength of the
271 correlation between RNA signal and epidemiological data, with a p -value of 0.05 or lower signifying
272 significance.

273

274 3. Results & discussion

275 3.1. Viral RNA recovery efficiency

276 The recovery through the concentration and extraction steps was quantified by spiking samples
277 with serial dilutions of inactivated VSV. The percent recoveries for VSV spiked in PGS and PCS were 8.4
278 $\pm 3.6\%$ and $9.3 \pm 4.9\%$, respectively. The recovery of the surrogate virus through both PCS and PGS
279 concentration and extraction was similar with all spiked-in quantities. Other recent studies investigating
280 surrogate virus recoveries following similar PEG concentration reported variable results for various
281 surrogates; $<6\%$ recovery of murine hepatitis virus (MHV) (Ye et al., 2016) along with reported recoveries
282 of $33.3 \pm 15.6\%$ and 57% of *Escherichia virus* MS2 (MS2) by Balboa et al. (2020) and Kumar et al.
283 (2020). Other concentration methods have also been used, such as ultrafiltration and ultracentrifugation
284 ($\sim 20\%$ to 33.5% recovery efficiency of MHV) (Ahmed et al., 2020b; Ye et al., 2016) and aluminum
285 hydroxide adsorption-precipitation ($30.4 \pm 11.0\%$ recovery of *Mengovirus* (MGV)) (Medema et al., 2020).
286 It is important to recognize that each study used slightly different methods and viral surrogates, making it
287 difficult to make direct comparisons and generalizations (Lu et al., 2020; Michael-Kordatou et al., 2020).
288 Each surrogate virus will differ in how it interacts with wastewater and this may also be dependent on the
289 characteristics of the wastewater as well as the properties of the virus/fragment that may have very
290 different partitioning/degradation characteristics. It is unclear yet how effective filtration-based
291 concentration techniques perform with high-solid samples, especially with viruses that are highly
292 associated with solids. When analyzing high solids containing samples, such as PGS and PCS, PEG
293 precipitation or other flocculation approaches may be more effective due to an incompatibility of this
294 matrix with ultrafiltration due to possible complication associated with membrane clogging. The
295 advantages of using PGS and PCS, which may have a greater and more consistent RNA signal, should
296 be balanced against the apparent lower recovery of PEG precipitation. Additional studies are needed to
297 develop and assess appropriate and effective methods and surrogates for analysis of SARS-Cov-2 in
298 wastewaters.

299

300 **3.2. Comparison of RT-qPCR and RT-ddPCR for the detection and** 301 **quantification of SARS-CoV-2 RNA**

302 This study tested the detection and quantification of RT-ddPCR and RT-qPCR for SARS-CoV-2
303 RNA signal in PGS and PCS samples. The in vitro transcribed RNA was observed to be reliably detected
304 with primer-probe RT-ddPCR assays to a limit of detection of 5 copies/reaction in both N1 and N2 RT-
305 ddPCR assays. This is consistent with the purported high sensitivity of the digital PCR technology. In vitro
306 transcribed viral RNA was detected to a limit of detection of 2 copies/reaction in both the N1 and N2 RT-
307 qPCR assays, (using the high sensitivity Bio-Rad One-Step Reliance Supermix (Bio-Rad, Hercules, CA)),
308 which was unexpected when comparing to the RT-ddPCR limit of detection. The standard curves utilized
309 for the quantification of different RNA targets for RT-qPCR are as follows: N1 (slope: -3.372, intercept:
310 38.184, R^2 : 0.972, E: 97.96%), N2 (slope: -3.179, intercept: 37.870, R^2 : 0.954, E: 106.32%), PMMV
311 (slope: -2.806, intercept: 39.142, R^2 : 0.968, E: 127.17%) and VSV (slope: -3.518, intercept: 39.846, R^2 :
312 0.995, E: 92.41%). The standard curves demonstrate good linearity for RT-qPCR in a range between 2 to
313 60 copies/reaction for N1 and N2, 1.4×10^2 to 3.6×10^4 copies/reaction for PMMV and 1.6×10^0 to $1.6 \times$
314 10^4 copies/reaction for VSV.

315 A comparison was performed between the one-step RT-qPCR and RT-ddPCR using the same
316 singleplex N1 probe-primer set for the quantification of SARS-CoV-2 in solids-rich, low concentration
317 SARS-CoV-2 RNA signal wastewaters (Figure 3). Six PGS samples and five PCS samples were analyzed
318 using RT-qPCR and RT-ddPCR. All samples were collected from the two cities during the same low
319 incidence periods (<60 active cases / 100,000 people) case number study period allowing the
320 assessment of quantification and degree of variability in samples with low RNA concentrations. The mean
321 and standard error of the PGS samples analyzed during the same period of low incidence cases are
322 133.4 ± 9.0 and 167.1 ± 25.6 N1 gene copies/100 μ L of extracted RNA for RT-ddPCR and RT-qPCR,
323 respectively. Meanwhile, the mean and standard error of the PCS samples are 33.5 ± 5.8 and $130.4 \pm$
324 20.8 gene copies/100 μ L of extracted RNA for RT-ddPCR and RT-qPCR, respectively (Figure 3).
325 Although a significant decrease in detected copies for PCS samples with RT-ddPCR is observed, it is

326 noted that the coefficient of variation (%CV) for the ddPCR assay (38.4%) compared to qPCR (35.7%).

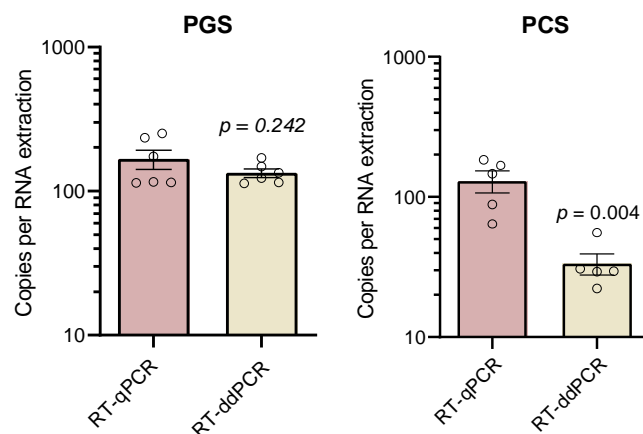


Figure 3: Comparison of copies per 100 µL of extracted RNA in RT-qPCR and RT-ddPCR for PGS (n=6) and PCS (n=5).

327 While the %CV for PGS samples for the ddPCR assay is lower (16.5%) compared to qPCR (37.5%).

328 The difference in quantification of the PCS samples between the N1 RT-qPCR and RT-ddPCR
329 assays suggests inhibition of the reverse transcription and/or polymerase chain reaction of the PCS
330 sample. Given that this assay partitions the sample volume into approximately 1 nL droplets, it's
331 conceivable that the effective concentration of any RT and/or PCR inhibitors present in the PCS matrix
332 are markedly increased. In contrast, RT-qPCR is performed in a non-partitioned assay volume and may
333 thus be less sensitive to inhibition. The apparent inhibition in ddPCR may also be explained by
334 differences in the reagents used for the RT-ddPCR and RT-qPCR assays. The inhibition
335 resistance/inhibitor removal of the high sensitivity RT-qPCR reagent appears to provide better detection
336 when utilized in pegged sludge matrices. Quantification of two-fold and five-fold dilutions of PCS samples
337 was performed and support the theory that RT-ddPCR was likely inhibited; RT-qPCR shows good
338 quantification of diluted samples while RT-ddPCR suffered from inhibition. These findings contradict the
339 theoretical assumption that RT-ddPCR is less prone to inhibition due to relative insensitivity to differences
340 in amplification efficiencies (due to its binary "all-or-nothing" reporting of amplification) (Salipante and
341 Jerome, 2020). However, at least one report found that undiluted raw wastewater inhibits one-step RT-
342 ddPCR amplification of PMMV RNA to the same degree as the RT-qPCR assay (Rački et al., 2014).

343 Given that RNA in both PGS and PCS samples was at a very low concentration, approaching the limits of
344 detection, it is highly likely that inhibitors in the PCS matrix are responsible for the decreased sensitivity
345 observed in RT-qPCR vs. RT-ddPCR.

346 Of note, it was also attempted in this study to use a commercially available multiplex RT-ddPCR
347 assay that employs primer-probe sets amplifying N1, N2 and N3 regions of the viral N RNA as well as a
348 human transcript (SARS-CoV-2, Bio-Rad). However, it was determined that the discrimination between
349 positive and negative droplets (fluorescence amplitude) was poor, making quantitative analysis
350 impossible. RT-ddPCR has a myriad of theoretical advantages such as absolute quantification that is not
351 dependent on calibration curves, insensitivity to common PCR inhibitors, and the ability to multiplex
352 (Salipante and Jerome, 2020). There is a need to explore this further in future studies and to optimize
353 these methods and quantification techniques for wastewater samples. However, based on the better
354 detection using the current RT-qPCR approach, this method was utilized for the remainder of this study to
355 quantify SARS-CoV-2 in both PGS and PCS solids from the Ottawa and Gatineau WRRFs.

356 **3.3. Detection and variance of SARS-CoV-2 viral RNA in PGS and PCS**

357 In this study, the sensitivity and variability of the RT-qPCR assay in PGS and PCS was compared
358 by investigating the percentage of sample replicates; with replicates including repeated RNA extraction
359 step and PCR quantification samples along with technical triplicates. The limit of detection used in the
360 study for RT-qPCR assays is described above. Replicate runs (24 paired PGS and PCS samples, for a
361 total of 72 technical replicates each) were collected on the same dates across 83 days. PCS samples
362 collected and analyzed at the same time as PGS samples over a 3-month period exhibited stronger
363 percent detection for N1 (92.7% for PCS compared to 79.2% for PGS, $p = 0.007$) and N2 (90.6% for PCS
364 compared to 82.3% for PGS, $p = 0.092$) (Figure 4). Variance in percent detection of PCS was shown to
365 be similar for all samples, with coefficients of variation ranging from 29.1% to 31.7%.

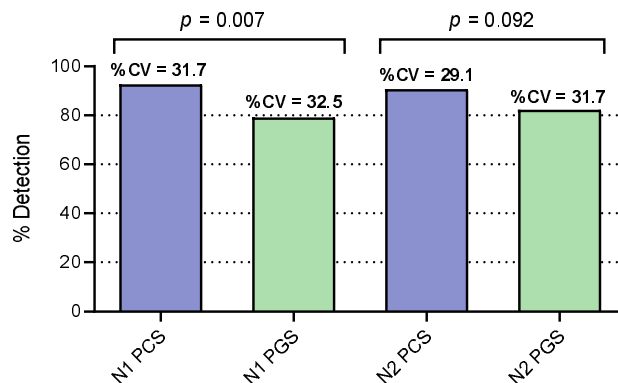


Figure 4: Sensitivity of N1 and N2 RT-qPCR assays comparison between PCS and PGS samples. Significance between detections established using Chi-Squared test. Variance is shown with %CV (n=24).

366

367 The decreased sensitivity of SARS-CoV-2 detection in PGS samples could be due to the
368 increased susceptibility of solid particulate matter in this wastewater fraction to daily fluctuations in
369 flowrate and wastewater biochemical characteristics at the WRRFs compared to the sludge samples
370 collected in the primary clarifier stream. In addition, the PGS samples undergo a laboratory settling step
371 in this study to isolate the settled solids from the liquid fraction of the sample. This additional step (which
372 is not applied to the PCS samples) may also contribute to the lower percent detection of SARS-CoV-2
373 signal of these samples due to increased holding times and processing times. As such, the result of this
374 study confirms PCS samples as the high-solids samples that demonstrate an elevated frequency of
375 detection of SARS-CoV-2 N1 and N2 RNA in municipal wastewaters during decreasing and low incidence
376 of community COVID-19 (Alpaslan-Kocamemi et al., 2020; Balboa et al., 2020; Peccia et al., 2020a). In
377 addition, it is noted that the viral RNA longitudinal trendline from the PGS samples did not show strong
378 correlation with either the trendline from the PCS samples, or municipal epidemiological data, further
379 supporting PCS sampling as the more robust basis for community COVID-19 monitoring in wastewater
380 solids.

381 3.4. Variability of normalization biomarkers

382 A multitude of systematic variations exist in molecular wastewater surveillance that makes it
383 challenging to accurately measure SARS-CoV-2 RNA across days, months and years. These include, but

384 are not limited to: diurnal variation in plant flow, changes in gross proportions of solids, sample collection
385 and storage, sample processing and sample analysis. Due to these factors, a critical aspect of
386 wastewater epidemiology is sample normalization (Armanious et al., 2016). The necessity to normalize
387 SARS-CoV-2 RNA data has also been identified in more recent studies (Alpaslan-Kocamemi et al., 2020;
388 Balboa et al., 2020; Kaplan et al., 2020; Peccia et al., 2020a; Wu et al., 2020). To compare the variability
389 and temporal consistency of biomarkers in this study 8 PCS samples (24 including technical triplicates)
390 were analyzed using RT-qPCR for all three biomarker gene regions: human-specific HF183 *Bacteroides*
391 16S rRNA, human eukaryotic 18S rRNA and PMMV. All three tested biomarkers were detected in PCS
392 samples with a relatively high level of incidence. While all three RNA targets were detected in PCS
393 samples, it was observed that the distribution of their expression (i.e. quantified through an analysis of
394 variance) of the fecal biomarker PMMV was lower as compared to the 16S and 18S biomarkers in PCS
395 samples (Figure 5 a). The lower variability of PMMV (C_t variance = 1.18) compared to 16S (C_t variance =
396 5.32) and 18S (C_t variance = 5.12) may be due to the relative toughness and stability of the virus in
397 difficult environments (Kitajima et al., 2018). Furthermore, the viral fragments of this biomarker may
398 preferentially adhere to the solids fraction of wastewaters via electrostatic and/or hydrophobic effects
399 (Armanious et al., 2016). Additionally, in order to quantify the variance of the normalization biomarkers in
400 this study, the samples run this comparison were also verified across each surveyed WRRF
401 independently (Figure 5b). The PMMV internal normalization biomarker shows an improved consistency
402 and lower variability (maximum change in C_t ; $\Delta C_t = 0.01$) between the WRRFs compared to 16S ($\Delta C_t =$
403 1.47) and 18S ($\Delta C_t = 2.30$); which demonstrates a relative steady signal between differing WRRFs. Due
404 to the consistency of the PMMV fecal biomarker in the PCS samples across 55 days of sampling, PMMV
405 was utilized in this study as a SARS-CoV-2 N1 and N2 RNA internal control for PCS samples. The low
406 variance of PMMV in PCS, coupled with the use of PMMV as an internal normalization biomarker, was
407 also recently reported by Wu et al. (2020).

408

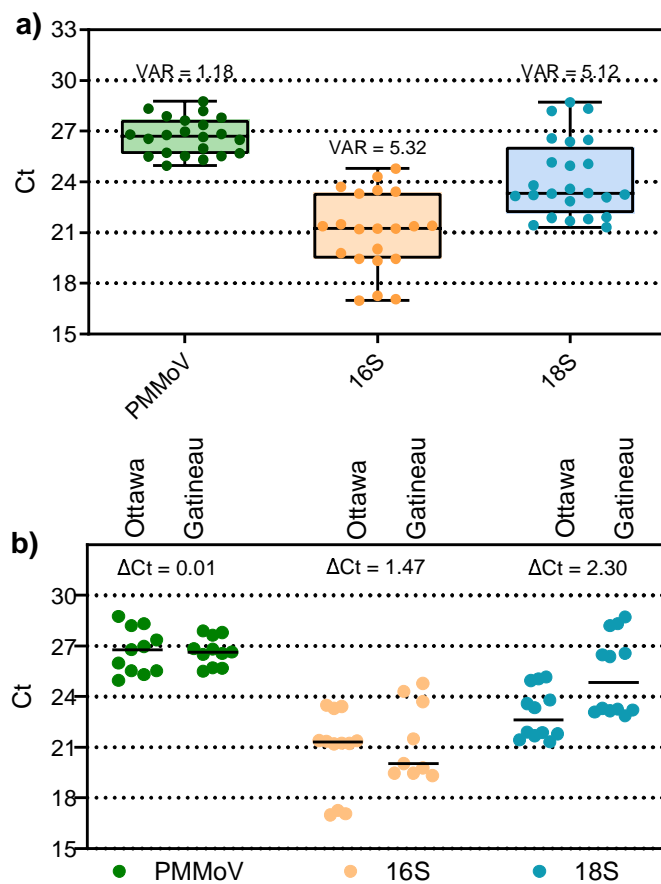


Figure 3: Variance of PCS normalization biomarkers, a) combined data set comprised of both cities samples, and b) data set separated by city. Analysis of variance and maximum change in C_t (ΔC_t) ($n=8$).

409

410

411 **3.5. Quantification of SARS-CoV-2 viral RNA in PCS and correlation with** 412 **COVID-19 case data**

413 As PCS was identified as the solids-rich sample showing the highest RNA detection rate, SARS-
414 CoV-2 RNA was measured in PCS samples from Ottawa and Gatineau WRRFs between April 1st and
415 June 30th, 2020. This sampling period encompasses a decreasing COVID-19 prevalence in two cities
416 (peaks of 56.7 and 57.3 confirmed cases/100K inhabitants in Ottawa and Gatineau respectively) as well
417 as an ensuing period of low prevalence characterized by many days with low new daily reported cases
418 (56.7 → 4.8 and 57.3 → 10.2 confirmed cases/100K inhabitants in Ottawa and Gatineau, respectively). In
419 addition to the technical triplicates of each sample, five of the 14 samples in Ottawa were re-extracted
420 and re-quantified via RT-qPCR. In Gatineau, four of the 8 samples were re-extracted and re-quantified via
421 RT-qPCR. Two distinct but complementary normalization approaches were applied to the observed
422 SARS-CoV-2 RNA signal to account for variations in WRRF wastewater flow, composition and treatment
423 along with temperature, time variations in travel and storage along with human errors in the processing of
424 the samples. In particular, this study normalizes the RNA signal for i) the WRRF mass flux of solids in the
425 sampled primary clarifier stream and ii) the PMMV internal normalization biomarker expression. The
426 SARS-CoV-2 viral RNA copies/L and the normalized viral data are benchmarked against and correlated
427 to epidemiological metrics provided by the Ottawa public health agency and the regional public health
428 agency of the city of Gatineau.

429 Three epidemiological data sets based on clinical testing were identified by the local public health
430 agencies as best estimates of COVID-19 prevalence in the two cities: i) daily new cases of COVID-19, ii)
431 active cases of COVID-19 based on an active period of fourteen days, and iii) percent positive of total
432 daily reported clinical COVID-19 tests performed. Two key factors/limitations are noted with respect to
433 these epidemiological data sets shown in this study. Firstly, the testing at the onset of the pandemic
434 (March and April 2020) was variable and low in both cities due to limitations in human resources,
435 laboratory reagents and testing equipment. Hence, the first four weeks of the twelve-week period for
436 which wastewater samples were profiled were subject to variable and lower testing rates per day that
437 likely under-reported both the number of new cases and active cases during this period. Secondly, early

438 testing/screening was less available to the general population in both cities, with testing heavily biased
439 towards hospitalized patients and health care workers. This potentially artificially inflates the percent
440 positive data during the first four weeks of the study, with the effect on the percent positive being likely
441 lesser than the effect of limited testing on the total case numbers.

442 ***SARS-CoV-2 RNA in PCS and correlation with COVID-19 case data***

443 The average and standard deviation of technical triplicates and extraction replicates that repeated
444 the concentration, extraction and RT-qPCR steps (shown as error bars in Figures 6 and 7) for the
445 longitudinal viral RNA data sets in this study are plotted along with a percent positive and seven day
446 floating average percent positive epidemiological data sets. Due to limited testing during the first four
447 weeks of the longitudinal study, percent positive was identified as a potentially useful epidemiological
448 metric of COVID-19 prevalence to compare to SARS-CoV-2 RNA measurements in wastewater. As such,
449 this metric is included in Figures 6 and 7 to be benchmarked against the measured SARS-CoV-2 signal.

450 N1 and N2 RNA signal is first expressed in copies/L (of PCS) in this study (Figures 6a and 7a).
451 Equivalent volumes of PCS were PEG concentrated and RNA extracted throughout the sampling period.
452 As expected, and similar to other studies investigating primary sludge and wastewater solids, the raw
453 copies/L data sets for the two cities (Figures 6a and 7a) are relatively noisy with no clear trend observed
454 (Medema et al., 2020; Randazzo et al., 2020; Wu et al., 2020). The observed concentrations in this study
455 (1.7×10^3 to 7.8×10^4 copies/L (Ottawa) and 6.6×10^4 to 3.8×10^5 copies/L (Gatineau)) are in agreement
456 with other studies investigating SARS-CoV-2 RNA viral signal in PCS. Concentration ranges of 1.7×10^6
457 to 4.6×10^8 copies/L, 1×10^4 to 4×10^4 copies/L and 1.2×10^4 to 4.0×10^4 copies/L have been reported in
458 PCS by Alpaslan-Kocamemi et al., (2020), Balboa et al., (2020) and Peccia et al., (2020b), respectively.

459 Although the N1 and N2 RNA genes show similar longitudinal trends to each other in both the
460 Ottawa and Gatineau WRRFs (Figures 6a and 7a), the inherent variations in signal results in noise,
461 making it difficult to identify real changes in viral signal. In particular, this is seen in the large amplitudes
462 of the standard deviations of many data points in the longitudinal data sets of Ottawa and Gatineau. The
463 noise in the RNA data may be caused by inherent, weather-induced random variations in wastewater

464 biochemical characteristics, solid composition and flowrate (e.g., due to weather, changes in daily
465 household water consumption, etc.) as well as potentially significant effects associated with the collection
466 and transport of the samples and RNA concentration, extraction and analysis. The copies/L longitudinal
467 data in Ottawa and Gatineau clearly demonstrate that SARS-CoV-2 quantification in wastewater is
468 inherently noisy and hence normalization of the data should be explored.

469 No significant correlation between N1 and N2 at either the Ottawa WRRF or the Gatineau WRRF
470 is observed across the study time period (Table 2). Strong and significant correlation would have
471 suggested that SARS-CoV-2 RNA might be intact in PCS prior to concentration and extraction, which is
472 not herein observed in this study. Critically, when comparing either N1 or N2 copies/L to each of the
473 epidemiological metrics (daily cases, active cases and percent positive) it appears that in Ottawa no
474 correlation exists between the N1 or N2 RNA copies/L signal and any of the three epidemiological
475 metrics. Meanwhile, in Gatineau, significant correlations exist between the N1 and N2 copies/L signal and
476 epidemiological data sets, with the strongest correlations being observed with the number of active cases
477 (Table 2).

478 ***Mass flux of primary clarified sludge copies SARS-CoV-2 RNA per day and correlation with***
479 ***COVID-19 case data***

480 To correct for systematic variability, the first normalization approach applied in this study is to
481 normalize the N1 and N2 RNA signal to both the mass of the PEG-concentrated solids subject to nucleic
482 acid extraction and also the daily mass flux (mass of volatile solids (VS) solids through the primary
483 clarifier stream per day) at each WRRF (Figures 6b and 7b). This normalization approach results in units
484 of N1 and N2 copies/day as a solids mass flux basis through the WRRF. This normalization approach is
485 intended to compensate for variations in solids concentration and flowrate in the primary clarifier stream
486 at the WRRF due to weather effects, precipitation and infiltration/inflow in the sewers.

487 When comparing longitudinal plots in Ottawa of copies/L (Figure 6a) to copies/d (Figure 6b), the
488 variance of the solids mass flux normalized data set of copies/d does not appear to have been
489 significantly reduced the systemic noise of the copies/L data sets. Similar findings are observed for the

490 Gatineau normalized data (Figures 7a and 7b). The substantial noise maintained in the solids mass flux
491 normalized data sets of the two cities and the significantly large standard deviations of longitudinal data
492 points indicates that the fluctuations associated with the solids concentration and flowrate in the primary
493 clarifier stream was likely not a dominant source of the inherent variance in the copies/L data sets.

494 As observed for the copies/L data, the correlation between the N1 and N2 data sets were not
495 significant for either Ottawa or Gatineau. Further, the normalization of the N1 and N2 data for solids mass
496 flux at the WRRFs appear to worsen correlations, with anticorrelations increasing, for all three
497 epidemiological metrics in Ottawa and Gatineau (Table 2). This lack of impact when normalizing
498 operational mass flux of solids at the two WRRFs in this study is likely due to the fact that both WRRFs
499 directly control the flow of the primary clarifier stream at their respective facilities, hence reducing the
500 variation in the flux of solids and in turn minimizing the impact of this variation in WRRF operation on the
501 N1 and N2 signal. Thus, systematic variation in the data sets are likely associated with the sample
502 collection and storage along with RNA concentration, extraction and analysis steps performed in the
503 study.

504 ***PMMV-normalized SARS-CoV-2 RNA in PCS and correlation with COVID-19 case data***

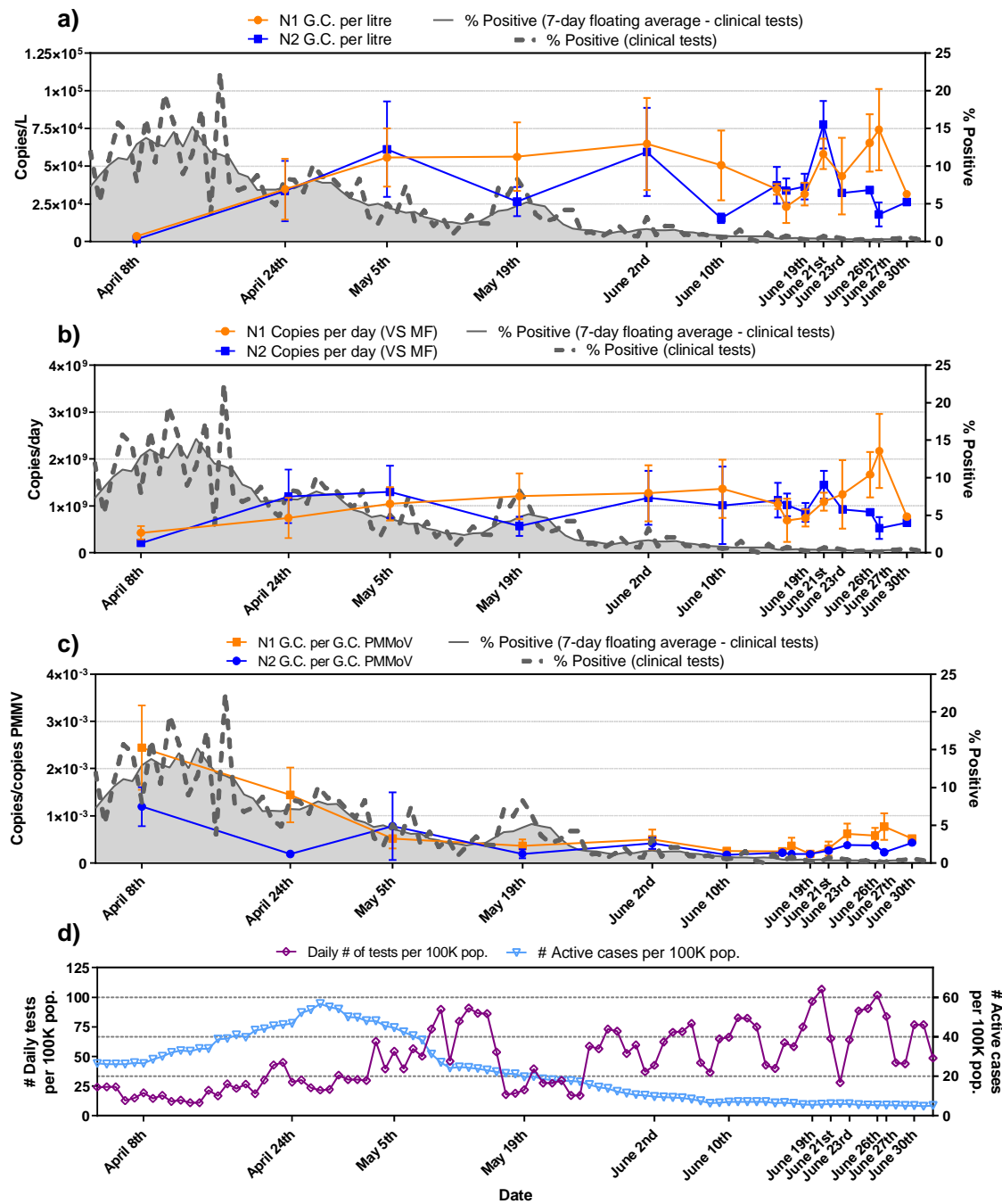
505 PMMV is the most abundant human fecal RNA virus (Kitajima et al., 2018) and has been
506 previously proposed as a biomarker for fecal contamination in water (Hamza et al., 2011; Rosario et al.,
507 2009). PMMV has also more recently been used as an internal reference for SARS-CoV-2 in wastewater
508 (Wu et al., 2020). The second normalization approach applied in this study is the division of the RNA N1
509 and N2 copies by PMMV copies. Due to its low variability and high expression in PCS, PMMV was
510 identified as the preferred internal reference of the three tested biomarkers tested in this study.

511 PMMV normalization appears to sufficiently reduce background noise associated with systematic
512 variations in the Ottawa and Gatineau WRRF RNA signals that are possibly associated with the collection
513 and transport of the samples along with the RNA concentration, extraction and analysis steps of PCS
514 RNA signal during decreasing and low incidence periods of COVID-19 disease in this study (Figure 6c
515 and 7c). In particular, the amplitude of the standard deviation associated with each data point in the

516 longitudinal data sets of Ottawa and Gatineau decreased. This increase in precision ultimately allows for
517 greater distinction between low-incidence data points, hence enabling improved identification of trends in
518 the data sets.

519 Correlation between the PMMV normalized N1 and N2 signals remained insignificant in Ottawa
520 and Gatineau (Table 2). However, this normalization approach also outlines strong, significant and
521 positive correlations between both the N1 gene and the N2 gene with all three epidemiological data sets
522 in Ottawa. The strongest correlation between N1 and N2 PMMV normalized RNA signal is observed with
523 the 7-day rolling average percent positive epidemiological metric in Ottawa. Although the percent positive
524 data during the first four weeks of the study may be biased towards hospitalized patients and health care
525 worker testing, this clinical testing metric in Ottawa is identified as the preferred metric by the public
526 health unit of the city (for the reasons described above). As such, decreasing the systematic variation in
527 the data sets via PMMV normalization establishes a modified trend of the RNA signal and this trend
528 shows the strongest correlation of the RNA signal to city's identified preferred epidemiological metric.

529 Strong, significant and positive correlation is also shown between the N1 PMMV normalized RNA
530 signal with the active cases epidemiologic metric in Gatineau; while the N2 PMMV normalized signal
531 shows moderate, significant correlation to the active cases. Although the PMMV normalized Gatineau
532 RNA signal data shows agreement with the active cases epidemiological metric, results were varied when
533 correlated to daily cases and 7-day rolling average percent positive. The strongest correlation observed in
534 this study for the Gatineau RNA signal and the epidemiological metrics of the City exists between both
535 the N1 and N2 copies/L RNA signal and the active cases. It is also noted that the longitudinal trends in N1
536 and N2 PMMV signals in Gatineau are similar to those in Ottawa. This is expected as the two cities are
537 geographically close with many inhabitants travelling across bridges between the cities. The observed
538 differences in correlations between SARS-CoV-2 RNA signal in wastewater to clinical testing metrics in
539 the two neighboring cities of this study is illustrative of the challenges associated with interpreting and
540 correlating RNA signal acquired from distinct WRRFs to clinical testing metrics acquired from distinct
541 health agencies.

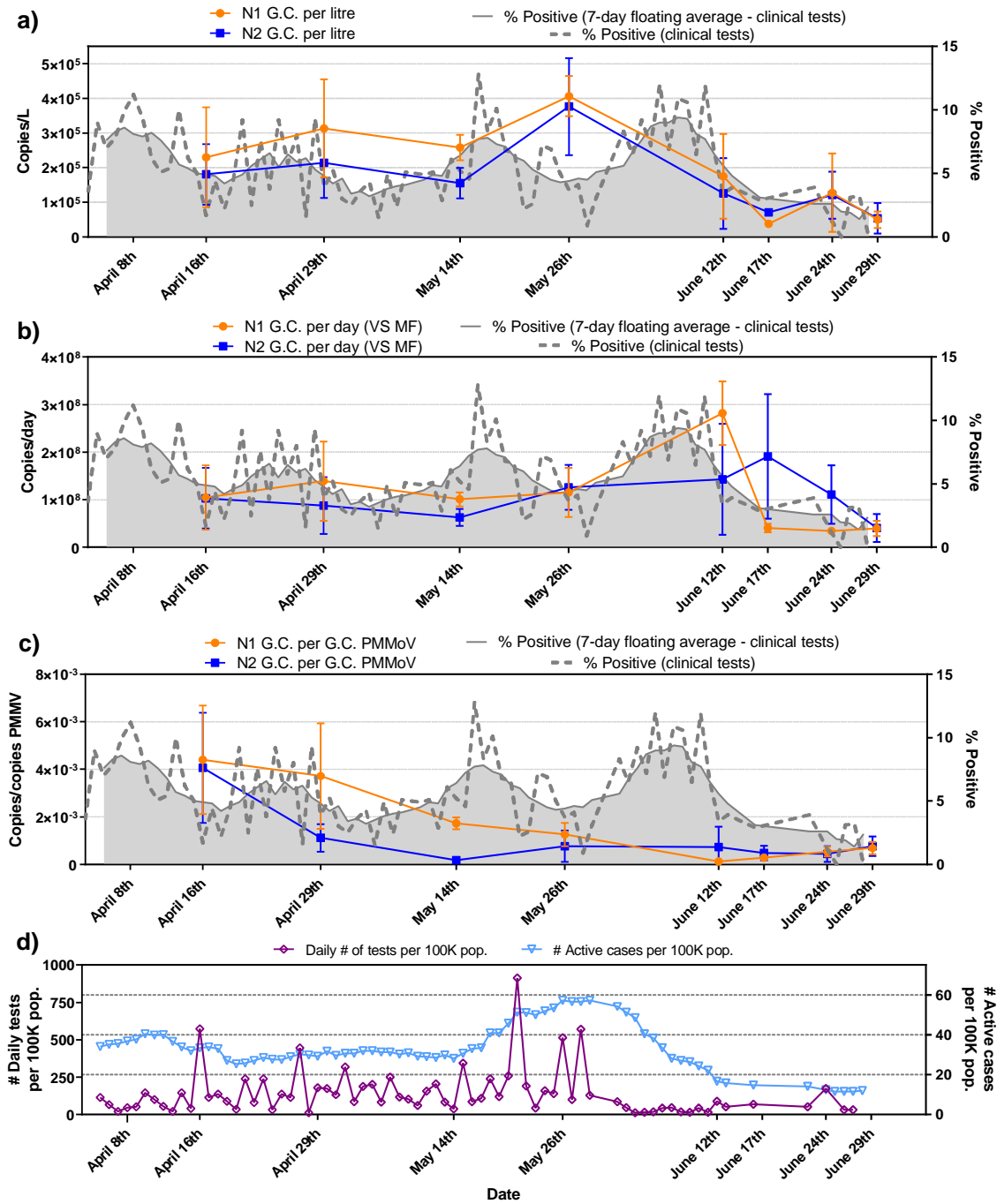


542

543 Figure 4: Trends of N1 and N2 SARS-CoV-2 viral copies with epidemiological metrics, a) copies/L of PCS, b)
 544 copies/d that was normalized by the mass flux through primary clarifier and c) copies/copies of PMMV that was
 545 normalized by PMMV.

546

547



548

549

Figure 5: Trends of N1 and N2 SARS-CoV-2 viral copies with epidemiological metrics, a) copies/L of PCS, b) copies/d that was normalized by the mass flux through primary clarifier and c) copies/copies of PMMV that was normalized by PMMV.

551

552

553

554

555 Table 2: Correlation analyses between SARS-CoV-2 RNA signal in PCS in the Ottawa and Gatineau WRRFs with
 556 epidemiological metrics. RNA signal is expressed as copies/L of PCS, copies/d that was normalized by the mass flux
 557 through primary clarifier, and copies/copies of PMMV that was normalized by PMMV.

			Copies/L	Copies/d Normalized by mass flux through plant	Copies/copies PMMV Normalized by copies of PMMV
Ottawa	N1 vs. N2	<i>p-value</i>	0.390	0.451	0.061
		R	0.880	0.808	0.469
	N1 vs. daily cases	<i>p-value</i>	<0.001	<0.001	0.049
		R	-0.209	-0.328	0.143
	N2 vs. daily cases	<i>p-value</i>	0.002	<0.001	0.003
		R	-0.140	-0.213	0.372
	N1 vs. active cases	<i>p-value</i>	<0.001	<0.001	0.003
		R	-0.233	-0.289	0.243
	N2 vs. active cases	<i>p-value</i>	0.002	<0.001	0.003
		R	-0.163	-0.163	0.350
	N1 vs. 7-day rolling average % positive	<i>p-value</i>	<0.001	<0.001	0.003
		R	-0.378	-0.238	0.498
	N2 vs. 7-day rolling average % positive	<i>p-value</i>	0.002	<0.001	0.049
		R	-0.323	-0.274	0.639
Gatineau	N1 vs. N2	<i>p-value</i>	0.063	0.983	0.201
		R	0.938	0.178	0.761
	N1 vs. daily cases	<i>p-value</i>	0.003	0.01	0.029
		R	0.399	-0.050	0.383
	N2 vs. daily cases	<i>p-value</i>	0.003	0.001	0.033
		R	0.140	-0.480	-0.144
	N1 vs. active cases	<i>p-value</i>	0.003	0.298	0.003
		R	0.919	0.125	0.483
	N2 vs. active cases	<i>p-value</i>	0.003	0.185	0.003
		R	0.950	-0.108	0.256
	N1 vs. 7-day rolling average % positive	<i>p-value</i>	0.003	0.008	0.123
		R	0.55	0.178	0.322
	N2 vs. 7-day rolling average % positive	<i>p-value</i>	0.003	<0.001	0.058
		R	0.364	-0.129	-0.022

558

559 **4. Conclusion**

560 This study is the first investigation and detection of SARS-CoV-2 trends in wastewater in Canada.
561 It identifies primary clarified sludge as a preferred solids-rich sample compared to post grit solids for the
562 detection of SARS-CoV-2 signal during decreasing and low incidence of viral load in communities. Based
563 on the reagents used in this study, RT-qPCR shows superior quantification of SARS-CoV-2 N1 and N2
564 gene signal in primary clarified sludge compared to RT-ddPCR. Finally, it is demonstrated that PMMV is a
565 potential effective normalization biomarker for RNA signal to reduce noise inherent to the WRRF
566 operation along with the sampling, transport and processing of the samples. The normalization of N1 and
567 N2 SARS-CoV-2 signal using PMMV enables strong correlation to epidemiological metrics in two
568 surveyed WRRFs across decreasing and low-incidence cases of COVID-19.

569 **Declaration of competing interests**

570 The authors declare that no known competing financial interests or personal relationships could
571 appear to influence the work reported in this manuscript.

572 **Acknowledgements**

573 The authors wish to acknowledge the help and assistance of the Dr. Marc-André Langlois of the
574 University of Ottawa, the Children's Hospital of Eastern Ontario's Research Institute, Ms. Tammy Rose,
575 Mr. Pawel Szulc and Mr. Tyler Hicks the City of Ottawa, Mr. Fabien Hollard of the City of Gatineau, Dr.
576 Monir Taha of Ottawa Public Health, Mr. François Tessier of le Centre intégré de santé et de services
577 sociaux de l'Outaouais (CISSSO), Public Health Ontario and l'Institut national de santé publique [Québec]
578 (INSPQ) and all their employees involved in the project during this study. Their time, facilities, resources
579 and assistance provided throughout the study greatly contributed to this work.

580

581 5. References

- 582 Ahmed, W., Angel, N., Edson, J., Bibby, K., Bivins, A., O'Brien, J.W., Choi, P.M., Kitajima, M., Simpson,
583 S.L., Li, J., Tschärke, B., Verhagen, R., Smith, W.J.M., Zaugg, J., Dierens, L., Hugenholtz, P.,
584 Thomas, K. V., Mueller, J.F., 2020a. First confirmed detection of SARS-CoV-2 in untreated
585 wastewater in Australia: A proof of concept for the wastewater surveillance of COVID-19 in the
586 community. *Sci. Total Environ.* 728, 138764. <https://doi.org/10.1016/j.scitotenv.2020.138764>
- 587 Ahmed, W., Bertsch, P.M., Bivins, A., Bibby, K., Farkas, K., Gathercole, A., Haramoto, E., Gyawali, P.,
588 Korajkic, A., McMinn, B.R., Mueller, J.F., Simpson, S.L., Smith, W.J.M., Symonds, E.M., Thomas, K.
589 V., Verhagen, R., Kitajima, M., 2020b. Comparison of virus concentration methods for the RT-
590 qPCR-based recovery of murine hepatitis virus, a surrogate for SARS-CoV-2 from untreated
591 wastewater. *Sci. Total Environ.* 739, 139960. <https://doi.org/10.1016/j.scitotenv.2020.139960>
- 592 Alpaslan-Kocamemi, B., Kurt, H., Sait, A., Sarac, F., Saatci, A.M., Pakdemirli, B., 2020. SARS-CoV-2
593 detection in Istanbul wastewater treatment plant sludges. *medRxiv* 2020.05.12.20099358.
594 <https://doi.org/10.1101/2020.05.12.20099358>
- 595 APHA, WEF, A., 2012. Standard methods for the examination of water and wastewater, 22nd ed. APHA,
596 WEF, AWWA, Washington, D.C.
- 597 APHA, 1989. Standard Methods, Standard methods for the examination of water and wastewater.
598 Washington, DC.
- 599 Armanious, A., Aeppli, M., Jacak, R., Refardt, D., Sigstam, T., Kohn, T., Sander, M., 2016. Viruses at
600 solid-water interfaces: A systematic assessment of interactions driving adsorption. *Environ. Sci.*
601 *Technol.* 50, 732–743. <https://doi.org/10.1021/acs.est.5b04644>
- 602 Balboa, S., Mauricio-Iglesias, M., Rodríguez, S., Martínez-Lamas, L., Vasallo, F.J., Regueiro, B., Lema,
603 J.M., 2020. The fate of SARS-CoV-2 in wastewater treatment plants points out the sludge line as a
604 suitable spot for incidence monitoring. *medRxiv* 2020.05.25.20112706.

- 605 <https://doi.org/10.1101/2020.05.25.20112706>
- 606 Bar-On, Y.M., Flamholz, A., Phillips, R., Milo, R., 2020. SARS-CoV-2 (COVID-19) by the numbers. *Elife* 9,
607 697–698. <https://doi.org/10.7554/eLife.57309>
- 608 Bar Or, I., Yaniv, K., Shagan, M., Ozer, E., Erster, O., Mendelson, E., Mannasse, B., Shirazi, R.,
609 Kramarsky-Winter, E., Nir, O., Abu-Ali, H., Ronen, Z., Rinott, E., Lewis, Y.E., Friedler, E.F., Paitan,
610 Y., Bitkover, E., Berchenko, Y., Kushmaro, A., 2020. Regressing SARS-CoV-2 sewage
611 measurements onto COVID-19 burden in the population: a proof-of-concept for quantitative
612 environmental surveillance. *medRxiv* 2020.04.26.20073569.
613 <https://doi.org/10.1101/2020.04.26.20073569>
- 614 Bernhard, A.E., Field, K.G., 2000. A PCR assay to discriminate human and ruminant feces on the basis of
615 host differences in *Bacteroides-Prevotella* genes encoding 16S rRNA. *Appl. Environ. Microbiol.* 66,
616 4571–4574. <https://doi.org/10.1128/AEM.66.10.4571-4574.2000>
- 617 Bustin, S.A., Benes, V., Garson, J.A., Hellemans, J., Huggett, J., Kubista, M., Mueller, R., Nolan, T.,
618 Pfaffl, M.W., Shipley, G.L., Vandesompele, J., Wittwer, C.T., 2009. The MIQE guidelines: Minimum
619 information for publication of quantitative real-time PCR experiments. *Clin. Chem.* 55, 611–622.
620 <https://doi.org/10.1373/clinchem.2008.112797>
- 621 Bwire, G.M., Majigo, M. V., Njiro, B.J., Mawazo, A., 2020. Detection profile of SARS-CoV-2 using
622 RT-PCR in different types of clinical specimens: a systematic review and meta-analysis. *J. Med.*
623 *Virol.* <https://doi.org/10.1002/jmv.26349>
- 624 CDC, 2020. Real-Time RT-PCR diagnostic panel for emergency use only. CDC EUA.
- 625 Comelli, H.L., Rimstad, E., Larsen, S., Myrmel, M., 2008. Detection of norovirus genotype I.3b and II.4 in
626 bioaccumulated blue mussels using different virus recovery methods. *Int. J. Food Microbiol.* 127,
627 53–59. <https://doi.org/10.1016/j.ijfoodmicro.2008.06.003>
- 628 Corman, V., Bleicker, T., Brünink, S., Drosten, C., Landt, O., Koopmans, M., Zambon Public Health

- 629 England, M., 2020. Diagnostic detection of 2019-nCoV by real-time RT-PCR. Charité Berlin.
- 630 Cureton, D.K., Massol, R.H., Whelan, S.P.J., Kirchhausen, T., 2010. The length of vesicular stomatitis
631 virus particles dictates a need for actin assembly during clathrin-dependent endocytosis. *PLoS*
632 *Pathog.* 6. <https://doi.org/10.1371/journal.ppat.1001127>
- 633 Dalzell, S., 2020. Australia to test sewage for coronavirus as testing net widens - ABC News [WWW
634 Document]. ABC News Aust. URL [https://www.abc.net.au/news/2020-04-17/australia-to-test-](https://www.abc.net.au/news/2020-04-17/australia-to-test-sewage-for-coronavirus-as-testing-net-widens/12156858)
635 [sewage-for-coronavirus-as-testing-net-widens/12156858](https://www.abc.net.au/news/2020-04-17/australia-to-test-sewage-for-coronavirus-as-testing-net-widens/12156858) (accessed 7.28.20).
- 636 Daughton, C.G., 2009. Chemicals from the practice of healthcare: challenges and unknowns posed by
637 residues in the environment. *Environ. Toxicol. Chem.* 28, 2490–2494. [https://doi.org/10.1897/09-](https://doi.org/10.1897/09-138.1)
638 [138.1](https://doi.org/10.1897/09-138.1)
- 639 Green, H.C., Haugland, R.A., Varma, M., Millen, H.T., Borchardt, M.A., Field, K.G., Walters, W.A., Knight,
640 R., Sivaganesan, M., Kelty, C.A., Shanks, O.C., 2014. Improved HF183 quantitative real-time PCR
641 assay for characterization of human fecal pollution in ambient surface water samples. *Appl. Environ.*
642 *Microbiol.* 80, 3086–3094. <https://doi.org/10.1128/AEM.04137-13>
- 643 Gundy, P.M., Gerba, C.P., Pepper, I.L., 2009. Survival of coronaviruses in water and wastewater. *Food*
644 *Environ. Virol.* 1, 10–14. <https://doi.org/10.1007/s12560-008-9001-6>
- 645 Gupta, S., Parker, J., Smits, S., Underwood, J., Dolwani, S., 2020. Persistent viral shedding of SARS-
646 CoV-2 in faeces – a rapid review. *Color. Dis.* 22, 611–620. <https://doi.org/10.1111/codi.15138>
- 647 Hamza, I.A., Jurzik, L., Überla, K., Wilhelm, M., 2011. Evaluation of pepper mild mottle virus, human
648 picobirnavirus and Torque teno virus as indicators of fecal contamination in river water. *Water Res.*
649 45, 1358–1368. <https://doi.org/10.1016/j.watres.2010.10.021>
- 650 Haramoto, E., Malla, B., Thakali, O., Kitajima, M., 2020. First environmental surveillance for the presence
651 of SARS-CoV-2 RNA in wastewater and river water in Japan. *Sci. Total Environ.* 737, 140405.
652 <https://doi.org/10.1016/j.scitotenv.2020.140405>

- 653 Hill, K., Zamyadi, A., Deere, D., Vanrolleghem, P.A., Crosbie, N.D., 2020. SARS-CoV-2 known and
654 unknowns, implications for the water sector and wastewater-based epidemiology to support national
655 responses worldwide: early review of global experiences with the COVID-19 pandemic. *Water Qual.*
656 *Res. J.* 1–11. <https://doi.org/10.2166/wqrj.2020.100>
- 657 ISO, 2017. ISO 15216-1:2017 - Microbiology of the food chain — Horizontal method for determination of
658 hepatitis A virus and norovirus using real-time RT-PCR — Part 1: Method for quantification.
- 659 Kaplan, E.H., Wang, D., Wang, M., Malik, A.A., Zulli, A., Peccia, J.H., 2020. Aligning SARS-CoV-2
660 Indicators via an epidemic model: Application to hospital admissions and RNA detection in sewage
661 sludge. *medRxiv* 2020.06.27.20141739. <https://doi.org/10.1101/2020.06.27.20141739>
- 662 Kitajima, M., Sassi, H.P., Torrey, J.R., 2018. Pepper mild mottle virus as a water quality indicator. *npj*
663 *Clean Water* 1. <https://doi.org/10.1038/s41545-018-0019-5>
- 664 Kumar, M., Patel, A.K., Shah, A. V., Raval, J., Rajpara, N., Joshi, M., Joshi, C.G., 2020. First proof of the
665 capability of wastewater surveillance for COVID-19 in India through detection of genetic material of
666 SARS-CoV-2. *Sci. Total Environ.* 709, 141326. <https://doi.org/10.1016/j.scitotenv.2020.141326>
- 667 La Rosa, G., Bonadonna, L., Lucentini, L., Kenmoe, S., Suffredini, E., 2020. Coronavirus in water
668 environments: Occurrence, persistence and concentration methods - A scoping review. *Water Res.*
669 179, 115899. <https://doi.org/10.1016/j.watres.2020.115899>
- 670 Lee, H.W., Lee, H.M., Yoon, S.R., Kim, S.H., Ha, J.H., 2018. Pretreatment with propidium
671 monoazide/sodium lauroyl sarcosinate improves discrimination of infectious waterborne virus by RT-
672 qPCR combined with magnetic separation. *Environ. Pollut.* 233, 306–314.
673 <https://doi.org/10.1016/j.envpol.2017.10.081>
- 674 Letchworth, G.J., Rodriguez, L.L., Barrera, J.D.C., 1999. Vesicular stomatitis. *Vet. J.* 157, 239–260.
675 <https://doi.org/10.1053/tvjl.1998.0303>
- 676 Long, Q.X., Tang, X.J., Shi, Q.L., Li, Q., Deng, H.J., Yuan, J., Hu, J.L., Xu, W., Zhang, Y., Lv, F.J., Su, K.,

- 677 Zhang, F., Gong, J., Wu, B., Liu, X.M., Li, J.J., Qiu, J.F., Chen, J., Huang, A.L., 2020. Clinical and
678 immunological assessment of asymptomatic SARS-CoV-2 infections. *Nat. Med.*
679 <https://doi.org/10.1038/s41591-020-0965-6>
- 680 Lowther, J.A., Bosch, A., Butot, S., Ollivier, J., Mäde, D., Rutjes, S.A., Hardouin, G., Lombard, B., in't
681 Veld, P., Leclercq, A., 2019. Validation of EN ISO method 15216 - Part 1 – Quantification of
682 hepatitis A virus and norovirus in food matrices. *Int. J. Food Microbiol.* 288, 82–90.
683 <https://doi.org/10.1016/j.ijfoodmicro.2017.11.014>
- 684 Lu, D., Huang, Z., Luo, J., Zhang, X., Sha, S., 2020. Primary concentration – The critical step in
685 implementing the wastewater based epidemiology for the COVID-19 pandemic: A mini-review. *Sci.*
686 *Total Environ.* 747, 141245. <https://doi.org/10.1016/j.scitotenv.2020.141245>
- 687 Medema, G., Heijnen, L., Elsinga, G., Italiaander, R., Brouwer, A., 2020. Presence of SARS-Coronavirus-
688 2 RNA in sewage and correlation with reported COVID-19 prevalence in the early stage of the
689 epidemic in the Netherlands. *Environ. Sci. Technol. Lett.* <https://doi.org/10.1021/acs.estlett.0c00357>
- 690 Michael-Kordatou, I., Karaolia, P., Fatta-Kassinos, D., 2020. Sewage analysis as a tool for the COVID-19
691 pandemic response and management: the urgent need for optimised protocols for SARS-CoV-2
692 detection and quantification. *J. Environ. Chem. Eng.* 8, 104306.
693 <https://doi.org/10.1016/j.jece.2020.104306>
- 694 National Institute for Public Health and the Environment, 2020. Sewage research: decline of novel
695 coronavirus in the Netherlands | RIVM [WWW Document]. RIVM. URL
696 <https://www.rivm.nl/en/news/sewage-research-decline-of-novel-coronavirus-in-netherlands>
697 (accessed 7.28.20).
- 698 Nemudryi, A., Nemudraia, A., Surya, K., Wiegand, T., Buyukyork, M., Wilkinson, R., Wiedenheft, B.,
699 2020. Temporal detection and phylogenetic assessment of SARS-CoV-2 in municipal wastewater.
700 *medRxiv* 2020.04.15.20066746. <https://doi.org/10.1101/2020.04.15.20066746>
- 701 Orive, G., Lertxundi, U., Barcelo, D., 2020. Early SARS-CoV-2 outbreak detection by sewage-based

- 702 epidemiology. *Sci. Total Environ.* 732, 139298. <https://doi.org/10.1016/j.scitotenv.2020.139298>
- 703 Pan, X., Chen, D., Xia, Y., Wu, X., Li, T., Ou, X., Zhou, L., Liu, J., 2020. Asymptomatic cases in a family
704 cluster with SARS-CoV-2 infection. *Lancet Infect. Dis.* 20, 410–411. [https://doi.org/10.1016/S1473-](https://doi.org/10.1016/S1473-3099(20)30114-6)
705 3099(20)30114-6
- 706 Parasa, S., Desai, M., Thoguluva Chandrasekar, V., Patel, H.K., Kennedy, K.F., Roesch, T., Spadaccini,
707 M., Colombo, M., Gabbiadini, R., Artifon, E.L.A., Repici, A., Sharma, P., 2020. Prevalence of
708 gastrointestinal symptoms and fecal viral shedding in Patients with coronavirus disease 2019: A
709 systematic review and meta-analysis. *JAMA Netw. open* 3, e2011335.
710 <https://doi.org/10.1001/jamanetworkopen.2020.11335>
- 711 Peccia, J., Zulli, A., Brackney, D.E., Grubaugh, N.D., Edward, H., Casanovas-massana, A., Ko, A.I.,
712 Malik, A.A., Wang, D., 2020a. SARS-CoV-2 RNA concentrations in primary municipal sewage
713 sludge as a leading indicator of COVID-19 outbreak dynamics 1.
- 714 Peccia, J., Zulli, A., Brackney, D.E., Grubaugh, N.D., Kaplan, E.H., Casanovas-Massana, A., Ko, A.I.,
715 Malik, A.A., Wang, D., Wang, M., Weinberger, D.M., Omer, S.B., 2020b. SARS-CoV-2 RNA
716 concentrations in primary municipal sewage sludge as a leading indicator of COVID-19 outbreak
717 dynamics. *medRxiv* 1, 2020.05.19.20105999. <https://doi.org/10.1101/2020.05.19.20105999>
- 718 Petterson, S., Grøndahl-Rosado, R., Nilsen, V., Myrmel, M., Robertson, L.J., 2015. Variability in the
719 recovery of a virus concentration procedure in water: Implications for QMRA. *Water Res.* 87, 79–86.
720 <https://doi.org/10.1016/j.watres.2015.09.006>
- 721 Pleitgen, F., 2020. Covid-19: Sewage could hold the key to stopping new coronavirus outbreaks - CNN
722 [WWW Document]. CNN. URL [https://www.cnn.com/2020/06/01/europe/germany-sewage-](https://www.cnn.com/2020/06/01/europe/germany-sewage-coronavirus-detection-intl/index.html)
723 coronavirus-detection-intl/index.html (accessed 7.28.20).
- 724 Rački, N., Dreo, T., Gutierrez-Aguirre, I., Blejec, A., Ravnikar, M., 2014. Reverse transcriptase droplet
725 digital PCR shows high resilience to PCR inhibitors from plant, soil and water samples. *Plant*
726 *Methods* 10, 1–10. <https://doi.org/10.1186/s13007-014-0042-6>

- 727 Randazzo, W., Truchado, P., Cuevas-Ferrando, E., Simón, P., Allende, A., Sánchez, G., 2020. SARS-
728 CoV-2 RNA in wastewater anticipated COVID-19 occurrence in a low prevalence area. *Water Res.*
729 181. <https://doi.org/10.1016/j.watres.2020.115942>
- 730 Rimoldi, S.G., Stefani, F., Gigantiello, A., Polesello, S., Comandatore, F., Mileto, D., Maresca, M.,
731 Longobardi, C., Mancon, A., Romeri, F., Pagani, C., Moja, L., Gismondo, M.R., Salerno, F., 2020.
732 Presence and vitality of SARS-CoV-2 virus in wastewaters and rivers. *medRxiv*
733 2020.05.01.20086009. <https://doi.org/10.1101/2020.05.01.20086009>
- 734 Rosario, K., Symonds, E.M., Sinigalliano, C., Stewart, J., Breitbart, M., 2009. Pepper mild mottle virus as
735 an indicator of fecal pollution. *Appl. Environ. Microbiol.* 75, 7261–7267.
736 <https://doi.org/10.1128/AEM.00410-09>
- 737 Salipante, S.J., Jerome, K.R., 2020. Digital PCR—an emerging technology with broad applications in
738 microbiology. *Clin. Chem.* 66, 117–123. <https://doi.org/10.1373/clinchem.2019.304048>
- 739 Thompson, J.R., Nancharaiyah, Y. V, Gu, X., Lin, W., Rajal, V.B., Haines, M.B., Girones, R., Ching, L.,
740 Alm, E.J., Wuertz, S., 2020. Making waves: Wastewater surveillance of SARS-CoV-2 for
741 population-based health management 184. <https://doi.org/10.1016/j.watres.2020.116181>
- 742 Wu, F., Zhang, J., Xiao, A., Gu, X., Lee, W.L., Armas, F., Kauffman, K., Hanage, W., Matus, M., Ghaeli,
743 N., Endo, N., Duvallet, C., Poyet, M., Moniz, K., Washburne, A.D., Erickson, T.B., Chai, P.R.,
744 Thompson, J., Alm, E.J., 2020. SARS-CoV-2 titers in wastewater are higher than expected from
745 clinically confirmed cases. *mSystems* 5, 2020.04.05.20051540.
746 <https://doi.org/10.1128/mSystems.00614-20>
- 747 Wurtzer, S., Marechal, V., Mouchel, J.-M., Maday, Y., Teyssou, R., Richard, E., Almayrac, J.L., Moulin, L.,
748 2020. Evaluation of lockdown impact on SARS-CoV-2 dynamics through viral genome quantification
749 in Paris wastewaters. *medRxiv* 2020.04.12.20062679. <https://doi.org/10.1101/2020.04.12.20062679>
- 750 Ye, Y., Ellenberg, R.M., Graham, K.E., Wigginton, K.R., 2016. Survivability, partitioning, and recovery of
751 enveloped viruses in untreated municipal wastewater. *Environ. Sci. Technol.* 50, 5077–5085.

752 <https://doi.org/10.1021/acs.est.6b00876>

753 Yle, 2020. THL to track coronavirus in waste water | Yle Uutiset | yle.fi [WWW Document]. Yle. URL
754 https://yle.fi/uutiset/osasto/news/thl_to_track_coronavirus_in_waste_water/11315440 (accessed
755 7.28.20).

756 Zhang, T., Cui, X., Zhao, X., Wang, J., Zheng, J., Zheng, G., Guo, W., Cai, C., He, S., Xu, Y., 2020.
757 Detectable SARS-CoV-2 viral RNA in feces of three children during recovery period of COVID-19
758 pneumonia. *J. Med. Virol.* 92, 909–914. <https://doi.org/10.1002/jmv.25795>

759

760

761

762

763

764

765

766

767

768

769

770

771

772

773 **Supplemental Material**

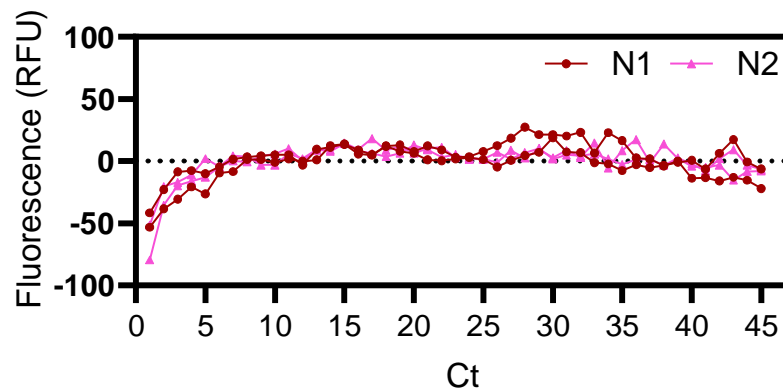


Figure S1: Amplification curves confirming that the bio-banked sample from Aug. 2019 (prior to pandemic) is a negative sample, quantified for the N1 and N2 SARS-CoV-2 genes.

774

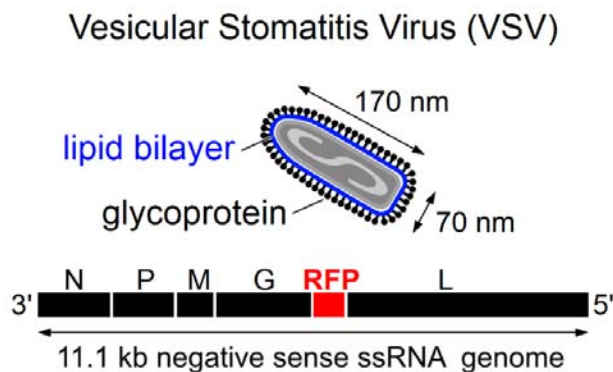


Figure S2: Schematic of VSV, lipid bilayer and glycoprotein identified.

775

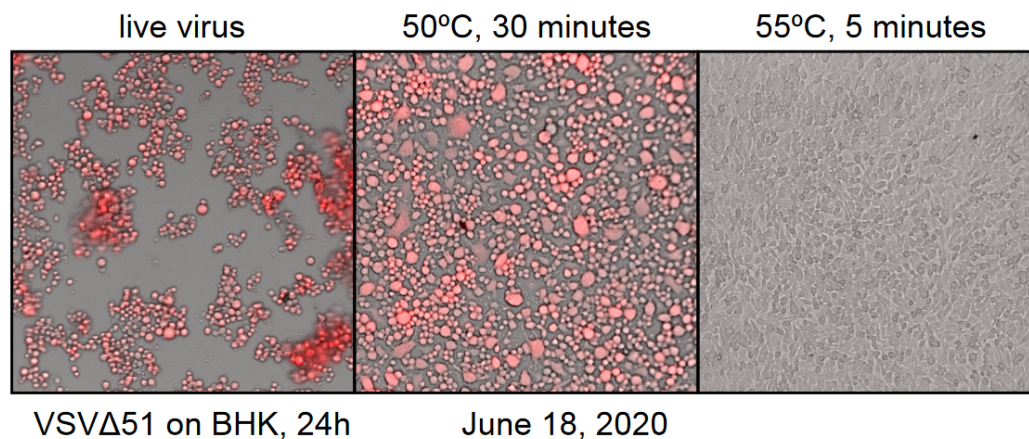


Figure S3: Confirmation of VSV heat inactivation.

776

777

778 Table S1: Average and standard deviations of wastewater quality characteristics of the PGS samples across the

Ottawa	PGS		Temp. (°C)	pH	DO (mg/L)	sBOD (mg/L)	sCOD (mg/L)	TAN (mg-N/L)	Turbidity (NTU)	TSS (mg/L)	VSS (mg/L)
		Average	16.75	7.41	4.05	7.81	70.04	19.22	129.79	162.39	153.83
		Standard deviation	3.47	0.23	1.48	5.32	15.55	16.20	44.28	73.12	70.95
Gatineau	PGS		Temp. (°C)	pH	DO (mg/L)	sBOD (mg/L)	sCOD (mg/L)	TAN (mg-N/L)	Turbidity (NTU)	TSS (mg/L)	VSS (mg/L)
		Average	15.46	7.43	4.96	7.60	73.38	12.19	128.22	144.77	129.88
		Standard deviation	4.96	0.25	2.05	3.90	23.89	10.99	99.34	125.80	113.64

779 study period.

780

781 Table S2: Average and standard deviations of wastewater quality characteristics of PCS samples across the study
782 period.

783

Ottawa	PCS		TS (g/L)	VS (g/L)	% VS
		Average	19.7	16.1	81.5
		Standard deviation	10.0	8.2	-
Gatineau	PCS		TS (g/L)	VS (g/L)	% VS
		Average	24.0	21.8	90.8
		Standard deviation	11.9	9.6	-

784

Table S3: List of PCR primer and probe sets.

Primer/probe & supplier	Sequence	Reference
2019-nCoV_N1 forward primer (IDT)	GAC CCC AAA ATC AGC GAA AT	(CDC, 2020)
2019-nCoV_N1 reverse primer (IDT)	TCT GGT TAC TGC CAG TTG AAT CTG	(CDC, 2020)
2019-nCoV_N1 probe (IDT)	6-FAM-ACC CCG CAT/ZEN/ TAC GTT TGG TGG ACC-IOWA BLACK FQ	(CDC, 2020)
2019-nCoV_N2 forward primer (IDT)	TTA CAA ACA TTG GCC GCA AA	(CDC, 2020)
2019-nCoV_N2 reverse primer (IDT)	GCG CGA CAT TCC GAA GAA	(CDC, 2020)
2019-nCoV_N2 probe (IDT)	6-FAM-ACA ATT TGC/ZEN/CCC CAG CGC TTC AG-IOWA BLACK FQ	(CDC, 2020)
2019-nCoV_N3 forward primer (IDT)	GGG AGC CTT GAA TAC ACC AAA A	(CDC, 2020)
2019-nCoV_N3 reverse primer (IDT)	TGT AGC ACG ATT GCA GCA TTG	(CDC, 2020)
2019-nCoV_N3 probe (IDT)	6-FAM/AYC ACA TTG/ZEN/GCA CCC GCA ATC CTG-IOWA BLACK FQ	(CDC, 2020)
Sarbeco_E forward primer (IDT)	ACA GGT ACG TTA ATA GTT AAT AGC GT	(Corman et al., 2020)
Sarbeco_E reverse primer (IDT)	ATA TTG CAG CAG TAC GCA CAC A	(Corman et al., 2020)
Sarbeco_E probe (IDT)	6-FAM-ACA CTA GCC ATC CTT ACT GCG CTT CG-IOWA BLACK FQ	(Corman et al., 2020)
Bacteroides 16S forward primer (HF183) (ABI)	ATC ATG AGT TCA CAT GTC CG	(Bernhard and Field, 2000)
Bacteroides 16S reverse primer (BacR287) (ABI)	CTT CCT CTC AGA ACC CCT ATC C	(Green et al., 2014)
Bacteroides 16S probe (BacP234) (ABI)	6-FAM/CTA ATG GAA CGC ATC CC-MGB	(Green et al., 2014)
PMMV forward primer (ABI)	GAG TGG TTT GAC CTT AAC GTT GA	(Lee et al., 2018)
PMMV reverse primer (ABI)	TTG TCG GTT GCA ATG CAA GT	(Lee et al., 2018)
PMMV probe (ABI)	6-FAM-CCT ACC GAA GCA AAT G-MGB	(Lee et al., 2018)
VSV forward primer (ABI)	ATA AGA TAC CGG GCT TGC AC	<i>This study</i>
VSV reverse primer (ABI)	ACA AAG ACA TGC CCG ACA C	<i>This study</i>
VSV probe (ABI)	6-FAM-CCA TGT TGT ATT TGG ACC C-MGB	<i>This study</i>
Eukaryotic 18S rRNA primers and probe (ThermoFisher)	<i>Proprietary</i> (ThermoFisher Assay ID: Hs03003631_g1)	N/A

785